

Comparison between three rock slope hazard assessment methodologies based on the Åknes case study from Norway



Oppikofer Thierry, Hermanns Reginald L.
Geological Survey of Norway, Trondheim, Norway
Jaboyedoff Michel, Derron Marc-Henri
University of Lausanne, Lausanne, Switzerland
Brideau Marc-André, Jakob Matthias, Sturzenegger Matthieu
BGC Engineering Inc., Vancouver, BC

ABSTRACT

This paper compares the input required, treatment of uncertainty, output, and limitations of three recently developed rock slope hazard assessment methodologies using the Åknes rockslide in Norway as a case study. The input parameters vary strongly between the methods by using the strain rate, various geological parameters such as development of critical structures and kinematic assessments, or a regional frequency analysis as starting point to which observations of deformation rates and other parameters are added. Consequently, the output varies and is qualitative, qualitative and quantitative, or quantitative, respectively. Only one method includes a consequence analysis. Finally, all methods suggest that the Åknes rock slope is unstable. Thus, results are comparable for this site suggesting that a combination of methods is preferable to ensure the quality of the outcome and the resulting decision making on disaster risk prevention. Additional comparison of other rock slope instabilities in different geological settings would be highly supportive for this conclusion.

RÉSUMÉ

Cet article compare les données requises, le traitement de l'incertitude, et les résultats et les limitations de trois récentes méthodes de l'analyse du danger d'éboulement rocheux. Ces méthodes sont utilisées pour l'évaluation de l'instabilité de Åknes, en Norvège. Les données requises varient d'une méthode à l'autre, selon qu'elles prennent en compte le taux de déformation, certains paramètres géologiques comme le développement de discontinuités défavorables, ou la fréquence régionale comme point de considération initiale. En conséquence, les résultats varient et sont présentés de manière qualitative, qualitative et quantitative, ou quantitative. Seule une méthode considère une analyse des conséquences. Toutes les méthodes suggèrent que le versant rocheux d'Åknes est critique. Les résultats sont donc comparables pour cet endroit, et suggèrent que l'utilisation de méthodes en parallèle garantit une certaine qualité des résultats et de la prise de décisions pour la prévention des risques. Pour confirmer le résultat de cette étude, il serait très utile de comparer ces méthodes sur d'autres instabilités rocheuses, dans des contextes géologiques différents.

1 INTRODUCTION

Rock avalanches usually occur only once at a given location, however, studies have documented that multiple failures from one unstable rock slope can occur. The recurrence interval of rock avalanches relates to the specific geological conditions on each slope. Return periods of 10s of thousands of years in the arid Andes of Argentina (Hermanns et al., 2001), over thousand of years in glaciated Canada and Norway (Mathews and McTaggart, 1978, Schleier et al., 2017), to several decades (Grimstad and Nesdal, 1990) to just weeks as in the case of the Randa failures in 1991 in Switzerland (Sartori et al., 2003) have been reported. Hermanns et al. (2006) discuss that the sudden change of the stress field in the rock slope likely causes new deformation to occur that can eventually result in a subsequent failure. However, the remnants of repeated failure from one slope may no longer be identifiable in the geological record. It is thus impossible to calculate a probability of occurrence for a specific slope based on repeated events, such as commonly done for debris flows, rock falls, or snow avalanches, that are

controlled by weather conditions, availability of weathered material on the slope and rock wall characteristics.

It is important, to consider multiple failures at the same slope. These are especially likely to occur on slopes that are divided into domains or zones based on the structural configuration (Booth et al., 2014), where the strain rate within the rock mass and/or the deformation rate varies over the unstable slope (Böhme et al., 2013, Oppikofer et al., 2017). For such slopes, different failure scenarios with different likelihood of failure are possible. Hence hazard, consequence and risk analyses need to be carried out for each possible failure scenario.

Unstable rock slopes can impact an area larger than that of the originating rock avalanche by damming streams in confined valleys or impacting water bodies and thus creating displacement waves. However, in this paper we focus on unstable rock slopes that can lead to rock avalanches as defined by Hungr et al. (2014) as extremely rapid (> 5 m/s), massive, flow-like motion of fragmented rock from a large rock slide or rock fall. Only rock slope failures with a volume greater than $1,000,000 \text{ m}^3$ were considered in this project. This corresponds to a volume

threshold commonly used in references for rock avalanches with high mobility (e.g., Hsü 1975).

This paper compares the required input, treatment of uncertainty, output, and limitations of three recently developed rock slope hazard assessment methodologies using the Åknes rockslide in Norway as a case study. This rock slope, shows a large variation in strain and deformation rate over the unstable area and makes a definition of different scenarios with different likelihood of failure necessary (Blikra et al., 2006; Oppikofer et al., 2009).

2 ÅKNES ROCKSLIDE

The Åknes rockslide is located on a south-facing, 30° to 40° steep slope in the Sunnlyvsfjord, Western Norway (Figure 1A). The rockslide stretches from the up to 30 m wide back-scarp at ~900 m.a.s.l. to the toe at ~100 m.a.s.l. (Figure 1B). A deeply eroded gully along a vertical NNW-SSE fault forms the western flank of the rockslide, whereas the eastern limit follows a moderately SW-dipping fault (Ganerød et al., 2008). The rockslide is mainly composed of medium-grained orthogneiss, which has a well-developed metamorphic foliation and typical mineral banding. The gneiss is affected by several isoclinal folds, but also by large open folds and undulations leading to variable foliation orientations (Jaboyedoff et al., 2011). The failure surfaces of the Åknes rockslide are mainly parallel to the metamorphic foliation dipping between 27° and 34° to the S to SE (Braathen et al., 2004; Ganerød et al., 2008), and are daylighting at the toe of the rockslide. Differences in displacements directions are shown to be related to changes in the orientation of the foliation (Jaboyedoff et al., 2011).

The rockslide can be divided into several sections limited by subvertical N-S fractures and several failure surfaces daylighting at different elevations (Blikra, 2008; Ganerød et al., 2008; Kristensen, 2017; NVE, 2018). Current failure scenarios include the whole Åknes rockslide (scenario A; area: 0.59 km²; volume: 54 million m³), and a failure limited to the western flank (scenario B; area: 0.22 km²; volume: 18 million m³) (Kristensen, 2017) (Figure 1B). Note that scenario A encompasses also scenario B. Other scenarios with different extents and volumes are however also possible (Ganerød et al., 2008; NVE, 2018). The most notable difference between scenarios A and B are the displacement rates measured continuously with a wide range of techniques (Blikra, 2008; Kristensen, 2017). Displacement rates range from not significant to <0.5 cm/year at the toe of scenario A, and from 1.5 to 3.5 cm/year in the middle and upper eastern part. Fastest displacement rates are recorded on a ridge in the upper western part with 6 to 8 cm/year (uppermost part of scenario A and B), whereas the middle and lower part of the western flank (scenario B) moves by approximately 5.5 cm/year (Kristensen, 2017) (Figure 1B). At least three smaller rockslides occurred from the western flank of Åknes in the past centuries (Kveldsvik et al., 2008) (Figure 1B).

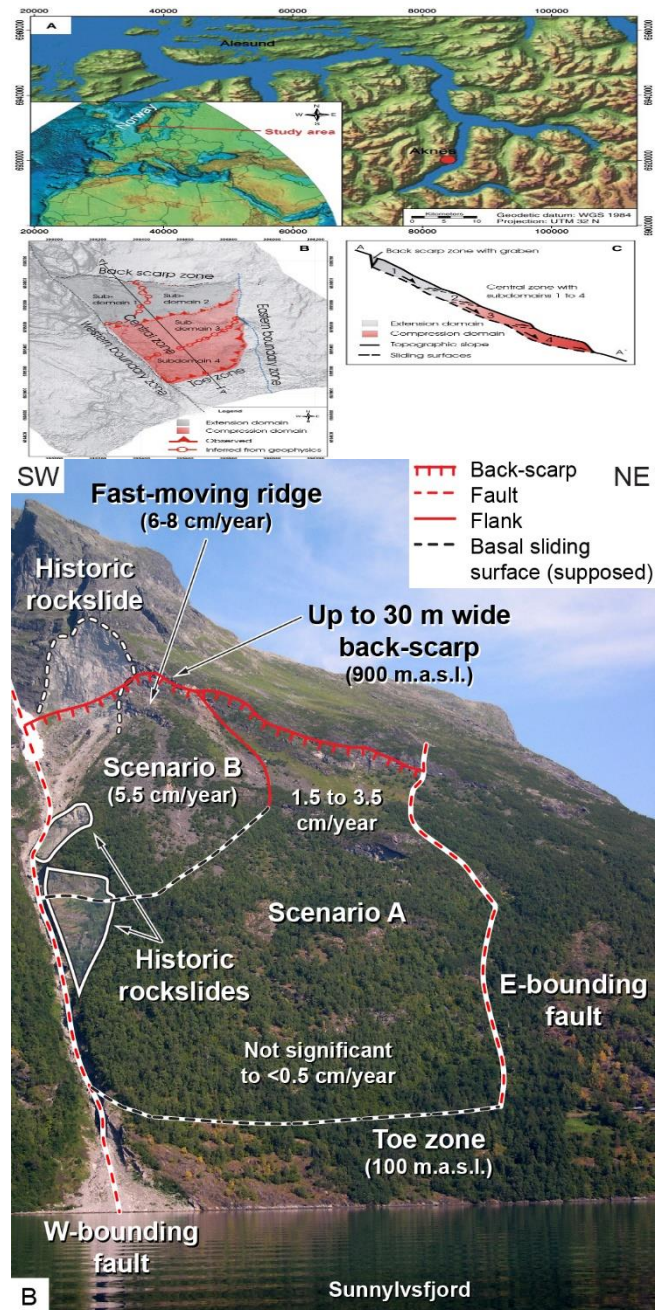


Figure 1. Location map and photograph of the Åknes rockslide: A) The rockslide is located in the Sunnlyvsfjord, western Norway; B) The picture shows the main rockslide features and current failure scenarios (A and B). The extent of historic rockslides (Kveldsvik et al., 2008) and current displacement rates of different parts of the slope (Kristensen, 2017) are shown (Photograph: L.H. Blikra).

3 Methodology

3.1 Assessment method by Jaboyedoff et al. (2012)

Where possible, a large rock slope instability assessment should include the following: 1) Delineation of the deformed/unstable area; 2) Volume estimates of unstable

The panel concluded that with today's scientific knowledge a large rock slope failure cannot be determined quantitatively (e.g. the rock slope will fail with a specific annual likelihood). It can, however, be predicted qualitatively. Therefore, the hazard and risk classification system was developed qualitatively, even though the consequence assessment is quantitative (Oppikofer et al. 2016a).

The hazard assessment is based on three geomorphological observations on the unstable rock slope (development of back scarp, lateral release surface, and underlying sliding surface), two engineering geological and structural criteria (orientation of penetrative sliding structures and kinematic feasibility tests), as well as displacement rates, acceleration of displacement rate, past events along the slope and other signs of activity (Figure 5, summarized from Hermanns et al. 2012, 2013). Scores are defined for each of these observations. The classification also allows to define the uncertainty of each observation relatively or normalized. The combination of the 9 criteria scores is summed and the uncertainty assessments are combined to yield an uncertainty estimate for the hazard assessment (Figure 5).

1. Back-scarp	Score	Likelihood
Not developed	0	0.0 %
Partly open over width of slide body (few cm to m)	0.5	0.0 %
Fully open over width of slide body (few cm to m)	1	100.0 %
2. Potential sliding structures	Score	Likelihood
No penetrative structures dip out of the slope	0	0.0 %
Penetrative structures dip on average < 20 degree or steeper than the slope	0.5	0.0 %
Penetrative structures dip on average > 20 degree and daylight with the slope	1	100.0 %
3. Lateral release surfaces	Score	Likelihood
Not developed	0	0.0 %
Partly developed on 1 side	0.25	0.0 %
Fully developed or free slope on 1 side or partly developed on 2 sides	0.5	16.7 %
Fully developed or free slope on 1 side and partly developed on 1 side	0.75	66.7 %
Fully developed or free slope on 2 sides	1	16.7 %
4. Kinematic feasibility test	Score	Likelihood
Kinematic feasibility test does not allow for planar sliding, wedge sliding or toppling	0	0.0 %
Failure is partly feasible kinematically	0.5	0.0 %
Failure is feasible kinematically	0.75	0.0 %
Failure is partly feasible kinematically on persistent discontinuities	0.75	0.0 %
Failure is feasible kinematically on persistent discontinuities	1	100.0 %
5. Morphologic expression of the rupture surface	Score	Likelihood
No indication on slope morphology	0	0.0 %
Slope morphology suggests formation of a rupture surface (bulging, convexity, springs)	0.5	40.0 %
Continuous rupture surface is suggested by slope morphology and can be mapped out	1	60.0 %
6. Displacement rates	Score	Likelihood
No significant movement	0	0.0 %
0.2 - 0.5 cm/year	1	0.0 %
0.5 - 1 cm/year	2	0.0 %
1 - 4 cm/year	3	20.0 %
4 - 10 cm/year	4	70.0 %
> 10 cm/year	5	10.0 %
7. Acceleration (if velocity is >0.5 cm/yr and <10 cm/yr)	Score	Likelihood
No acceleration or change in displacement rates	0	90.0 %
Increase in displacement rates	1	10.0 %
8. Increase of rock fall activity	Score	Likelihood
No increase of rock fall activity	0	0.0 %
Increase of rock fall activity	1	100.0 %
9. Past events	Score	Likelihood
No post-glacial events of similar size	0	0.0 %
One or several events older than 5000 years of similar size	0.5	100.0 %
One or several events younger than 5000 years of similar size	1	0.0 %

Figure 5. Nine criteria are categorized for the hazard assessment. The first 5 focus on morphological signs of deformation and rock slope engineering observations. The next two consider deformation rates and the change of these rates over time, and the last two focus on the activity of the rock slope. Uncertainties can be given to all these observations. The data shown here represent Åknes scenario B.

The Norwegian building codes guidelines are quantitative and defined in safety classes S1-S3 which dictates what kind of building can be constructed in an area with a yearly landslide likelihood of 1/100 (S1), 1/1,000 (S2), and 1/5,000 (S3). Therefore, the qualitative hazard assessment was divided into four hazard classes > 1/100 (S1), >1/1,000 (S2), > 1/5,000 (S3), and <1/5,000 by definition (Blikra et al., 2016). This definition is based on three considerations: 1) Norway has experienced historically 2-3 larger rock slope failures per century with loss of life, thus the number of sites plotting in the highest class should be lower. 2) the risk matrix is logarithmic and the values for the classes S2 and S3 can be calculated from the definition of class S1. 3) a slope that is not deforming today should have a yearly likelihood of failure >1/5,000 following the classification.

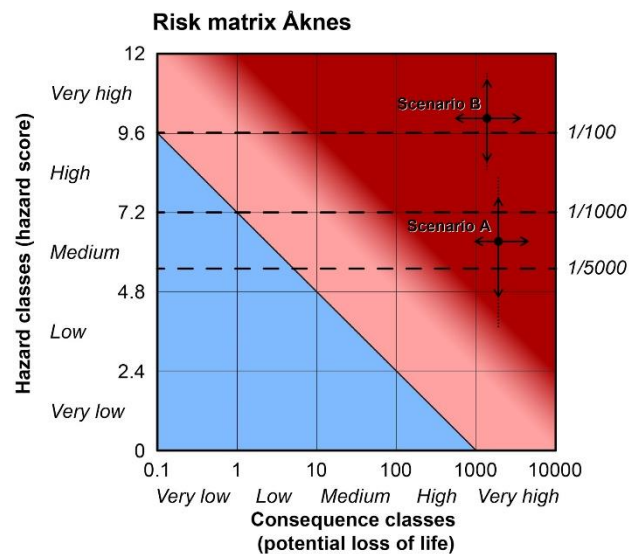


Figure 6. Risk matrix of the Åknes rockslide based on the hazard assessment method by Hermanns et al. (2012, 2013) along with the consequences assessment method by Oppikofer et al. (2016a, b). Yearly probabilities of failure associated with the hazard assessment are shown as dashed lines, as defined by Blikra et al. (2016).

The consequence assessment is focused on loss of life. It combines volume estimation for the unstable rock slope and its scenarios, a run-out analysis, a landslide dam analyses that includes the assessment of the upstream and potential downstream flood in cases where a rockslide dams a valley, a stability assessment of the potential dam and a displacement wave analysis in cases where a rock slope failure could impact a water body. In both the run-out and the displacement wave propagation area the possible loss of life is considered following a standardized procedure (Oppikofer et al. 2016a, 2016b, 2018). Also, the consequence analyses include an uncertainty analysis as the exposure of people in the hazard zone varies. The result of the combined hazard and risk analysis is plotted in a risk matrix which provides uncertainty margins for hazard and risk (Figure 6).

3.3 Assessment Method by Brideau et al. (2017)

The methodology proposed by Brideau et al. (2017) is based on desktop, field and laboratory analyses to estimate a range of rock avalanche frequencies for a specific slope. The first step consists of compiling a regional inventory of rock-avalanche deposits within an area of approximately 1,250 km² centered on the slope of interest and encompassing a variety of geological groups and formations. The area of terrain with a slope less than 20° (as it has a low potential to generate rock avalanche) is subtracted from the total inventory area to estimate a regional rock avalanche frequency (f-regional) over a series of concentric circle with radii of 5, 10, 15, and 20 km (Figure 7 and Table 1). The variation of rock avalanche intensity between the different circle area provides a first-order characterization of the influence of the regional-scale geology or tectonic structures on the spatial distribution of rock avalanches (i.e. is the study area located in a region with above average rock avalanche density?). Fjord regions such as the Storfjord study area have a subaerial and a submarine component to their inventory (Figure 7).

In regional-level study, it is not possible to review whether the submarine landslide deposit is the result of a rock avalanche that initiated subaerially or from submarine sediment.

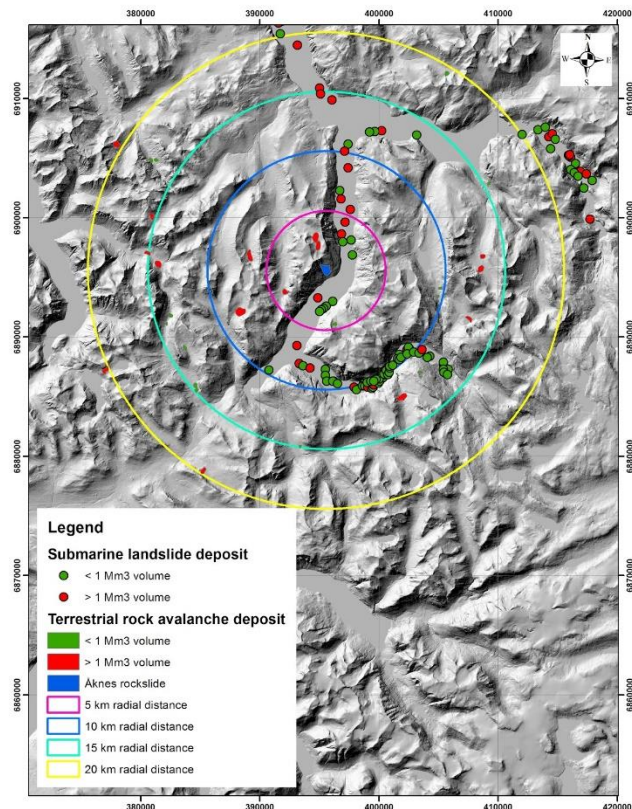


Figure 7. Distribution of rock avalanche with volume greater than 1 Mm³ in the area around the Åknes rockslide. The concentric circles were used to calculate rock avalanche density as a function of distance around the study area (Table 1).

Table 1. Large (> 1 Mm³) landslides (terrestrial and marine) density as a function of the distance from the Åknes rockslide.

Radius of circle centered on Åknes rockslide (km)	Number of large terrestrial landslides	Number of large terrestrial and submarine landslides	Area minus slope less than 20° (km ²)	Large terrestrial landslide density (event / km ²)	Large terrestrial and submarine landslide density (event / km ²)
5	3	6	46	0.065	0.13
10	5	16	177	0.028	0.090
15	10	20	394	0.025	0.051
20	15	26	719	0.020	0.036

The exhaustion, steady-state decline and constant frequency are the three main models that have been used to describe the temporal distribution of landslides after the last deglaciation (Cruden and Hu, 1993; Ballantyne et al. 2014). The recent work of Böhme et al. (2015) and Hermanns et al. (2017) in Norway suggest that, based on carbon and cosmogenic dating along with seismo-stratigraphy of landslide deposits, landslides were more frequent in the first 1,000 to 3,000 year after deglaciation (with large portion of the fjords being ice free starting around 12,500 years B.P.) but have since an approximately constant probability of occurrence. The work of Böhme et al. (2015) in the Storfjord region, which includes the study area for this project, suggests that 80% (16 of 20 landslides in their inventory) occurred in the last 10,000 years.

In the next step, the f-regional is scaled for the area occupied by the slope of interest providing f-specific. For the Åknes rockslide these two areas correspond to scenario A and scenario B.

In the final step, the f-specific values are further adjusted, if necessary based on field observations and measurements, to account for site specific kinematics conditions, evidence of recent or ongoing large-scale deformation, and evidence for the presence of potential permafrost (permafrost degradation over time due to climate change could decrease overall rock slope stability). The information available based on the desktop analyses (literature review, geomorphic mapping, potential failure scenario, and kinematic analyses), fieldwork (borehole log, photogrammetry, outcrop mapping, geomorphic observations, displacement monitoring) and laboratory testing (shear strength, uniaxial compressive strength, along with cosmogenic and radiocarbon dating) is subsequently used for adjusting the f-regional to the slope-specific conditions.

The magnitude of the potential adjustments below is subjective and should reflect the observed site conditions and knowledge of the important regional controls on rock slope stability. It should also be carried out by a team of experts, rather than a single researcher or practitioner. In this paper, the site-specific conditions considered include:

- Increasing f-specific by a factor of five when a feasible failure mechanism has been identified on a non-pervasive and persistent discontinuity set.
- Increasing f-specific by one order of magnitude when a feasible failure mechanism has been

identified in association with a pervasive and persistent discontinuity set or when the same discontinuity set and slope orientations have led to a nearby rock avalanche.

- Increasing f-specific by one order of magnitude when widespread deformation features without signs of recent activity or when localized deformation features with signs of recent activity has been identified.
- Increasing f-specific by two orders of magnitude when widespread deformation features with signs of recent activity has been identified or ongoing minor rock fall events are reported.
- Consider increasing f-specific by a factor of two to account for increasing intensity and amount of precipitation projected by climate change scenario where permafrost is not anticipated
- Consider increasing f-specific by one order of magnitude to account for the permafrost degradation projected by climate change scenarios.

4 RESULTS

4.1 Results for method by Jaboyedoff et al. (2012)

Two different scenarios for Åknes rockslide are assessed with this method. Scenario A corresponds to the larger rock avalanche volume. The rock mass considered is 937 m long and moves at 1.5 to 3.5 cm/year (Figure 1). Scenario B moved by 16 cm over a 520 m long scarp in one year. For both cases, movements occur at the top and at the toe. It is unclear if the whole movement at the top is matched by the same rate of movement at the toe. Some of the deformation appears to develop internally. In this case, the classification would be between the case next to last and last columns (2-1 and 2-2 in Figure 2). For scenario B the strain rate is 0.03% and for the scenario A 0.003%. In Figure 4, scenario A is located in the zone of High Medium-High scenario, and scenario B is High.

4.2 Results from the Method by Hermanns et al. (2012)

A statistical distribution is used to represent the variability of the calculated hazard score (Figure 6). This variability represents the combination of uncertainty estimated for each of the 9 input parameters (Figure 5). The results of the risk matrix (Figure 6) show that scenario A has a medium to high hazard with a mean likelihood that falls in class S3 (1/1,000 to 1/5,000) but the range of uncertainty reaches into class S2 (1/100 to 1/1,000). Based on the input shown in Figure 5, scenario B has a high to very high hazard with a corresponding mean yearly likelihood just above 1/100 years.

The consequence for both scenarios A and B is considered to be very high due to the displacement wave potential to be generated by the debris entering the fjord. Scenario A, with its greater volume, can generate a larger wave which can potentially lead to a greater number of fatalities. This is reflected by scenario A plotting to the right of scenario B on the consequence axis. The uncertainty associated with the consequence is related to uncertainty

of exposure of person that might be in the area of impact during the event and is represented by a minimum, mean, and maximum estimate for the potential loss of life for each scenario. This estimation is for an event without warning and evacuation as a baseline. A continuously monitoring early warning system now exists at Åknes that will lead to warning and timely evacuation in case of rock mass movement acceleration (Blikra 2008).

The combination of the hazard and consequence assessment suggests that both rock avalanche scenarios are considered to represent a high risk.

4.3 Results for the Method by Brideau et al. (2017)

The regional rock avalanche inventory highlights that the Åknes rockslide is within a rock avalanche "hot spot" as suggested by the increasing density per decreasing area of the concentric circles (Table 1). Using the temporal relationship by Böhme et al. (2015) and the rock avalanche density in the 5 km circle, a f-regional value of approximately 5×10^{-6} event/km²/year (3 rock avalanche \times 0.8 / 46 km² / 10,000 years) is estimated for the area nearest to Åknes rockslide. This value is multiplied by the area of Scenario A (0.22 km²) and Scenario B (0.59 km²) to provide a first estimate of the f-specific.

For both scenarios A and B, the f-specific is then adjusted by three orders of magnitude because there is a kinematically feasible failure mechanism on a pervasive and persistent discontinuity set, and documented ongoing movement over most of the extent of the potentially unstable rock mass. Accounting for the area of each scenario, the estimated f-specific (or probability of occurrence) is between 1/150 and 1/300 for scenario A and 1/450 and 1/900 for scenario B. A probability range is reported using only the terrestrial rock avalanches as the lower bound and the combined terrestrial and submarine large landslides as the upper bound. The large submarine landslide deposits could include subaerial rock avalanche that entered the fjord and large landslides that initiated in fine-grained submarine sediment at this level of analysis it is not known how many of each is present in the inventory.

Table 2. Summary of the rock slope assessment based on the three methods considered in this paper.

Rock Slope Assessment Method	Hazard Rating	Probability of Occurrence
Jaboyedoff et al. 2012	High-medium (A) High (B)	N/A
Hermanns et al. 2012	High-medium (A) Very-high (B)	1/1,000 to 1/5,000 (A) 1/100 (B)
Brideau et al. 2017	N/A	1/150 to 1/300 (A) 1/450 to 1/900 (B)

5 DISCUSSION

The results from the Jaboyedoff et al., (2012) and Hermanns et al., (2012) are consistent for both rock avalanche scenarios with scenario B representing the higher hazard while the method by Brideau et al. (2017) suggest that scenario A has the higher probability of

occurrence. The difference in these results is due to the greater sensitivity of the method by Hermanns et al. (2012) to the displacement rates whereas the method by Brideau et al. (2017) has a greater sensitivity to the area which could generate a rock avalanche greater than 1 Mm³. The methodology by Hermanns et al. (2012) leverages the available displacement monitoring data by having five displacement rate classes versus the two landslide activity classes in the method by Brideau et al. (2017). The methodology by Brideau et al. (2017) was developed to provide probability of occurrence estimate for slopes that did not have monitoring data available and instead leverages the regional history of rock avalanches.

The method by Hermanns et al. (2012) provides a more complete characterization of a potentially unstable slope by evaluating its hazard, consequence (including those associated with secondary hazards), risk and provides an estimate of the probability of occurrence. This method can be applied in different stages of an investigation to assess which geological condition requires additional attention to reduce uncertainties. So far, this method has been applied at various potentially unstable slopes to evaluate their hazard and risk (Blikra et al., 2016; Hermanns et al., 2016). That said the method by Hermanns et al. (2012) does not consider the spatial distribution of the deformation like in Jaboyedoff et al. (2012), nor the spatial distribution of nearby post-glacial rock avalanches like in Brideau et al. (2017). A comparison of the results from the three methods can provide an additional characterization of parameters that could influence a potentially unstable slope.

6 CONCLUSIONS

This paper compared the hazard assessment and probability of occurrence estimates for the Åknes rockslide in Norway using three methodologies. The input for each methodology included geomorphic mapping, geological model, kinematic analysis, rock fall activity, displacement monitoring, deformation pattern, regional DEM, and regional inventory of rock avalanche. The analysis considered two failure scenarios (A: whole slope failure, B: failure of fast moving section of the slope). The three methodologies found both scenarios to represent a medium high to very high hazard and the probability of occurrence to be greater than 1\5,000 for scenario A and greater than 1\1,000 for scenario B. We conclude that for locations with high risk of life loss or severe potential for infrastructure damage or loss, a combination of methods discussed will provide a range of results that could inform a hazard and risk assessment. This range is preferable than reliance on a single method, as rock avalanches do not lend themselves to traditional frequency analysis based on repeat events at the same location. The range in outcomes also provides a convenient sensitivity analysis that can be carried through a risk assessment and which would add credibility to the expert's judgement. Ultimately, we hope that combining these methods in decision making will reduce potential life loss by supporting monitoring and early warning systems for high risk situations.

7 REFERENCES

- Ballantyne, C.K. Sandeman, G.F., Stone, J.O., Wilson, P., 2014. Rock-slope failure following Late Pleistocene deglaciation on tectonically stable mountainous terrain. *Quaternary Science Reviews* 86: 144-157.
- Blikra, L.H., Majala, G., Anda, E., Berg, H., Eikennes, O., Helgas, G., Oppikofer, T., Hermanns, R., Bohme, M., 2016. Fare- og risikoklassifisering av ustabile fjellparti. Prepared by Norges vassdrags- og energidirektorat, Report Number 77-2016. 145 pp.
- Blikra, L. H. 2008. The Åknes rockslide; monitoring, threshold values and early warning. In: Chen, Z., Zhang, J.-M., Ho, K., Wu, F.-Q. & Li, Z.-K. (eds) *Proceedings of the 10th International Symposium on Landslides and Engineered Slopes*, Xi'an, China. pp. 1089-1094.
- Blikra, L. H., Anda, E., Høst, J. & Longva, O. 2006. Åknes/Tafjord prosjektet: Sannsynlighet og risiko knyttet til fjellskred og flodbølger fra Åknes og Hegguraksla. *Norges geologiske undersøkelse Report 2006.039*, 20.
- Böhme, M., Oppikofer, T., Longva, O., Jaboyedoff, M., Hermanns, R.L., Derron, M.-H., 2015. Analyses of past and present rock slope instabilities in a fjord valley: Implications for hazard estimations. *Geomorphology* 248: 464-474.
- Böhme, M., Hermanns, R.L., Oppikofer, T., Fischer, L., Bunkholt, H.S., Eiken, T., Pedrazzini, A., Derron, M.-H., Jaboyedoff, M., Blikra, L.H., 2013. Analyzing complex rock slope deformation at Stampa, western Norway, by integrating geomorphology, kinematics and numerical modeling. *Engineering Geology* 154, 116-130.
- Booth, A.M., Dehls, J., Eiken, T., Fischer, L., Hermanns, R.L., Oppikofer, T., 2014. Integrating diverse geologic and geodetic observations to determine failure mechanisms and deformation rates across a large bedrock landslide complex: the Osmundneset landslide, Sogn og Fjordane, Norway. *Landslides*, 1-12.
- Braathen, A., Blikra, L.H., Berg, S.S. & Karlsen, F., 2004. Rock-slope failures in Norway; type, geometry and hazard. *Norwegian Journal of Geology*, 84: 67-88.
- Brideau, M.-A., Jakob, M., McDougall, S., 2017. Methodology to estimate the rock avalanche frequency for a specific slope. In: *Abstracts of the 4th Slope Tectonics Conference*, Kyoto, Japan, p. 29.
- Chigira, M. 2009. September 2005 rain-induced catastrophic rockslides on slopes affected by deep-seated gravitational deformations, Kyushu, southern Japan. *Engineering Geology* 108: 1-15.
- Cruden, D.M., Hu, X.-Q., 1993. Exhaustion and steady state models for predicting landslide hazards in the Canadian Rocky Mountains. *Geomorphology* 8: 279-285.
- Ganerød, G.V., Grøneng, G., Rønning, J.S., Dalsegg, E., Elvebakk, H., Tønnesen, J.F., Kveldsvik, V., Eiken, T., Blikra, L.H. and Braathen, A., 2008. Geological model of the Åknes Rockslide, western Norway. *Engineering Geology* 102: 1-18.
- Grimstad, E., Nesdal, S., 1990. Loen rockslides: A historical review. *Norwegian Geotechnical Institute Publication 182*: 1-6.

- Hermanns, R.L., Schleier, M., Bohme, M., Blikra, L.H., Gosse, J., Ivy-Ochs, S., Hilger, P., 2017. Rock-avalanche activity in W and S Norway peaks after the retreat of the Scandinavian Ice Sheet. In: Proceedings of the 4th World Landslide Forum, Ljubljana, Slovenia, pp. 331-338.
- Hermanns, R.L., Oppikofer, T., Bohme, M., Dehls, J.F., Yugsi Molina, F.X., Penna, I.M., 2016. Rock slope instabilities in Norway: First systematic hazard and risk classification of 22 unstable rock slopes from northern, western and southern Norway. In: Aversa S, Cascini L, Picarelli L, Scavia C (eds) *Landslides and Engineered Slopes: Experience, Theory and Practice*. CRC Press, Rome, pp. 1107 - 1114.
- Hermanns, R.L., Oppikofer, T., Anda, E., Blikra, L.H., Böhme, M., Bunkholt, H., Crosta, G.B., Dahle, H., Devoli, G., Fischer, L., Jaboyedoff, M., Loew, S., Sætre, S., Yugsi Molina, F., 2013. Hazard and risk classification system for large unstable rock slopes in Norway. In: Genevois R, Prestininzi A, (eds) *International conference on Vajont - 1963-2013*. Italian Journal of Engineering Geology and Environment, Book series 6, DOI 10.4408/IJEGE.2013-06.B-22, Rome, Italy, p. 245-254.
- Hermanns, R.L., Oppikofer, T., Anda, E., Blikra, L.H., Bohme, M., Bunkholt, G., Crosta, G.B., Dahle, H., Devoli, G., Fischer, L., Jaboyedoff, M., Loew Simon, Saetre, S., Yugsi Molina, F., 2012. Recommended hazard and risk classification system for large unstable rock slopes in Norway. NGU report 2012.029, Geological Survey of Norway, Trondheim.
- Hermanns, R.L., Blikra, L.H., Naumann, M., Nilsen, B., Panthi, K.K., Stromeyer, D., Longva, O., 2006. Examples of multiple rock-slope collapses from Kofels (Ötz valley, Austria) and western Norway, *Engineering Geology* 83: . 94-108.
- Hermanns, R.L., Niedermann, S., Garcia, A.V., Gomez, J.S., Strecker, M.R., 2001. Neotectonics and catastrophic failure of mountain fronts in the southern intra-Andean Puna Plateau, Argentina. *Geology* 29, 619-622.
- Hsü, K.J., 1975. Catastrophic debris streams (sturzstroms) generated by rockfalls. *GSA Bulletin* 86: 129-140.
- Hungr, O., Leroueil, S., Picarelli, L., 2014. The Varnes Classification of landslide types, an update. *Landslides* 11: 167-194.
- Jaboyedoff, M., Derron, M.-H., Pedrazzini, A., Blikra, L.H., Crosta, G.B., Froese, C.R., Hermanns, R.L., Oppikofer, T., Bohme, M., and Stead, D. 2012. Fast assessment of susceptibility of massive rock instabilities. In *Proceedings of the 11th International Symposium on Landslides and Engineered Slopes*. Banff, Canada, pp. 459-465.
- Jaboyedoff, M., Oppikofer, T., Derron, M.-H., Blikra, L.H., Bohme, M., Saintot, A., 2011. Complex landslide behaviour and structural Control: a three-dimensional conceptual model of Åknes rockslide, Norway. In: *Slope Tectonics*. Geological Society, London, Special Publications 351: 147-161.
- Kristensen, L., 2017. Åknes status and overview. Presentation at Åknes Workshop, 30-31 January 2017, Oslo, Norway. Norwegian Water Resources and Energy Directorate, 75 p. Available at: <https://www.nve.no/Media/5460/l-kristensen-%C3%A5knes-overview-status-februar-2017.pdf>
- Kveldsvik, V., Nilsen, B., Einstein, H. and Nadim, F. (2008) Alternative approaches for analyses of a 100,000 m³ rock slide based on Barton-Bandis shear strength criterion. *Landslides*, 5, 2, 161-176.
- Mathews, W.H., and McTaggart, K.C. 1978. Hope rockslides, British Columbia, Canada. In *Rockslides and Avalanches*, Edited by B., Voight. Elsevier, pp. 259-275.
- NVE, 2018. Hazard zones for the Åknes rockslide, https://www.nve.no/Media/4974/%C3%A5kneset_v4.pdf, Accessed February 13, 2018.
- Oppikofer, T., Jaboyedoff, M., Blikra, L.H., Derron, M.H., 2009. Characterization and monitoring of the Åknes rockslide using terrestrial laser scanning. *Natural Hazards and Earth System Sciences* 9, 1003-1019.
- Oppikofer, T., Nordahl, B., Bunkholt, H., Nicolaisen, M., Jarna, A., Iversen, S., Hermanns, R.L., Bohme, M., Yugsi Molina, F.X., 2015. Database and online map service on unstable rock slopes in Norway - From data to perpetuation to public information. *Geomorphology* 249: 69-81.
- Oppikofer, T., Böhme, M., Nicolet, P., Penna, I., Hermanns, R.L., 2016a, *Metodikk for konsekvensanalyse av fjellskred*. NGU report 2016.047, Geological Survey of Norway, Trondheim, 67 p.
- Oppikofer, T., Hermanns, R.L., Sandøy, G., Böhme, M., Jaboyedoff, M., Horton, P., Roberts, N.J., Fuchs, H., 2016b. Quantification of casualties from potential rock-slope failures in Norway. In: Aversa S, Cascini L, Picarelli L, Scavia C (eds) *Landslides and Engineered Slopes: Experience, Theory and Practice*. CRC Press, Rome, pp. 1537–1544.
- Oppikofer, T., Saintot, A., Hermanns, R., Böhme, M., Scheiber, T., Gosse, J., Dreiås, G., 2017. From incipient slope instability through slope deformation to catastrophic failure - Different stages of failure development on the Ivasnasen and Vollan rock slopes (western Norway). *Geomorphology* 289, 96-116.
- Oppikofer, T., Hermanns, R.L., Roberts, N.J., Böhme, M., 2018, *SPLASH - Semi-empirical prediction of landslide-generated displacement wave run-up heights*, in press.
- Sartori, M., Baillifard, F., Jaboyedoff, M., Rouiller, J.-D., 2003. Kinematics of the 1991 Randa rockslides (Valais, Switzerland). *Natural Hazards and Earth System Science* 3: 423-433.
- Schleier, M., Hermanns, R.L., Gosse, J.C., Oppikofer, T., Rohn, J., Tønnesen, J.F., 2017. Subaqueous rock-avalanche deposits exposed by post-glacial isostatic rebound, Innfjorddalen, Western Norway. *Geomorphology* 289, 117-133.